J Mater Sci (2007) 42:8053–8061
DOI 10.1007/s10853-007-1680-0

POLYMER FIBERS 2006

Interfacial stress transfer in an aramid reinforced thermoplastic elastomer

A. B. Coffey · C. M. O'Bradaigh · R. J. Young

Received: 24 September 2006 / Accepted: 9 March 2007 / Published online: 29 June 2007

Abstract The interfacial micromechanics of Twaron 2200 aramid fibers in an engineering thermoplastic elastomer (Pebax 7033, polyether amide block co-polymer) has been investigated by determining the distribution of interfacial shear stress along fibers in single-fiber model composites using Raman spectroscopy. The effects of various fiber surface treatments on the interfacial shear stress and fragmentation of the aramid fibers are discussed. The fiber average stress increased linearly with applied matrix stress up to first fracture. Each composite was subjected to incremental tensile loading up to full fragmentation, while the stress in the fiber was monitored at each level of the applied stress. It was shown that the experimental approach allowed us to discriminate between the strengths of the interfaces in the different surface-treated aramid fiber Pebax matrix systems, but also to detect different phenomena (interfacial debonding, matrix yielding and fiber fracture) related intimately to the nature of stress transfer in composite materials. The efficacy of the surface treatments was clear by comparing the maximum interfacial shear stress with the fragment lengths of the modified aramid fibers. The fiber breaks observed using Raman spectroscopy were not clean breaks as observed with carbon or glass fibers, but manifested themselves as apparent breaks by fiber skin failure. The regions of fiber fracture were also investigated using optical microscopy.

A. B. Coffey · R. J. Young (✉)
Materials Science Centre, School of Materials, University of Manchester, Grosvenor Street, Manchester M1 7HS, UK
e-mail: Robert.young@manchester.ac.uk

A. B. Coffey · C. M. O'Bradaigh
Composite Research Unit, National University of Ireland, Galway, Ireland

Introduction

Aramid fibers have a unique combination of stiffness, strength, toughness and thermal resistance that the fibers suitable for reinforcement in many applications such as in the production of aircraft, automobiles, sporting goods, and more recently, medical devices [1]. However, a drawback restricting the use of aramid fibers is poor adhesion with most polymeric matrices due to their inert chemical structure and smooth surface, which prevents chemical and mechanical bonding to various substrates [2].

The behavior of composite materials is, in part, controlled by the nature of the interface, which in polymer-matrix composites is usually required to be strong thus imparting efficient load transfer from the matrix to the fibers. The quality and characteristics of the fiber/matrix interface needs to be addressed. It is generally accepted that there are three main factors important in determining the fiber/matrix adhesion: (i) covalent bonds between the fiber and matrix (chemical bonding), (ii) wettability of the fiber by the matrix (physical bonding); (iii) micromechanical interlocking. There have been many reviews of the methods used to evaluate and improve the interfacial shear strengths of composite materials [3–5]. For the most-part, however, the literature available for a thermoplastic elastomer reinforced with aramid fibers is quite scarce. The stress-transfer mechanisms between the matrix and fiber, and the interfacial properties for reinforced thermoplastic materials are becoming exceptionally important due to their ease of fabrication and reduced costs of manufacture.

Experimental stress or strain transfer profiles along the fiber in a polymer matrix can be obtained by employing the technique of Raman spectroscopy. This technique is based on the fact that the Raman frequencies of the atomic vibrations of commercial reinforcing fibers such as aramid

or carbon are stress dependent [6]. In this work, the application of Raman spectroscopy in the deformation of aramid-thermoplastic elastomeric composites has made it possible to obtain fundamental information about the micromechanics of the fiber/matrix interface, by monitoring the point-to-point variation in fiber stress or strain.

A number of mechanical tests have been developed to determine the effective adhesion and stress transfer from the matrix to a fiber in a composite. The most commonly-used tests on single-fiber composites are the fiber fragmentation test, the micro-debond test, and the single fiber pull-out test [7]. The fiber fragmentation test was used in this work due to the ease of manufacture of the samples. Aramid fibers historically have not been suitable for the fragmentation test using conventional methods. It is necessary for a fiber to break within the transparent matrix, and this break must be visible using microscopy techniques. Yet, for aramid fibers, to date it has not been possible to induce a fiber break in an epoxy matrix (which is the most commonly-studied matrix use). The reason for this is that Epoxy is a brittle thermoset material in which the elongation at failure is 1.5–2.5% [8]. The fiber failure strain for an aramid fiber is found to be greater than 2.7%. Thus, it was not possible for previous studies in which epoxy matrix was used to apply sufficient strain to the matrix in order to generate fiber fracture. For the fragmentation test to be successful, a matrix material with a larger ultimate strain than the fiber used is required. Thermoplastic elastomers have a failure strain of ca. 400%, thus it is possible to apply sufficient strain to the matrix, and therefore to the fiber, in order to induce fiber fragmentation.

In this present study the surfaces of the aramid fibers were modified using a variety of methods. Model composites containing single fibers were loaded in a Raman spectrometer. The data obtained has been used to assess the effect of surface treatment on the interfacial behavior of model composites made from the treated fibers and a thermoplastic elastomer matrix. It was found that multiple fragmentation occurred on increasing matrix load and that the fragment lengths were dependent on the surface treatments.

Experimental

Materials

The fiber used in this study was Twaron 2200 a poly (*p*-phenylene terephthalamide) (PPTA) aramid fiber, supplied by Akzo Nobel Research (Arnhem). The fibers have modulus E_f = 136 GPa, tensile strength, σ^*_f = 3.6 GPa and a failure strain ε^*_f = 2.6%. A Hitachi S-4700 Field Emission Scanning electron microscope (SEM) was used to determine fiber diameters. At least 20 fibers were selected randomly and then examined at three different magnification levels. Average diameters and standard deviations were calculated and the average fiber diameter and standard deviation was found to be 12.1 ± 0.5 μm.

The matrix used was a thermoplastic elastomer, polyether amide block co-polymer supplied by Atofina known commercially as 'Pebax'. These thermoplastic elastomers (TPE) consist of linear chains of hard polyamide (PA) blocks covalently linked to soft polyether (PE) blocks via ester groups. The molecular weight of the PE blocks varies from about 400–3,000 g/mol and that of the PA blocks varies from about 500–5,000 g/mol. These poly(ether-block-amides) are synthesized via a metallic $Ti(OR)_4$ catalyst which facilitates the melt polycondensation of carboxylic acid terminated amide blocks with polyoxyalkylene glycols.

The grade of Pebax used was Pebax 7033, with a modulus E_m = 128 MPa, yield stress σ_y = 32 MPa, Yield strain ε_y = 25%, ultimate failure stress σ^*_m = 67 MPa and an ultimate strain ε^*_m = 400%. A typical stress–strain curve for Pebax 7033 is shown in Fig. 1.

Fiber surface treatments

The fibers used in this study were subjected to a variety of surface treatments in order to attempt to improve the interfacial stress transfer between fiber and matrix. Details of the various surface treatments are given in Table 1.

Chemical Modification of the fiber surface was carried out. Chloride end-groups were grafted to the Twaron 2200 fibers using a variation of the method proposed by Andreopoulos [9]. A 5% w/w solution of methacryloyl chloride in carbon tetrachloride was added to the aramid fibers in which they sat for 1 h. The same procedure was used for succinyl chloride. The carbon tetrachloride was removed by evaporation at 40 °C and the fibers were

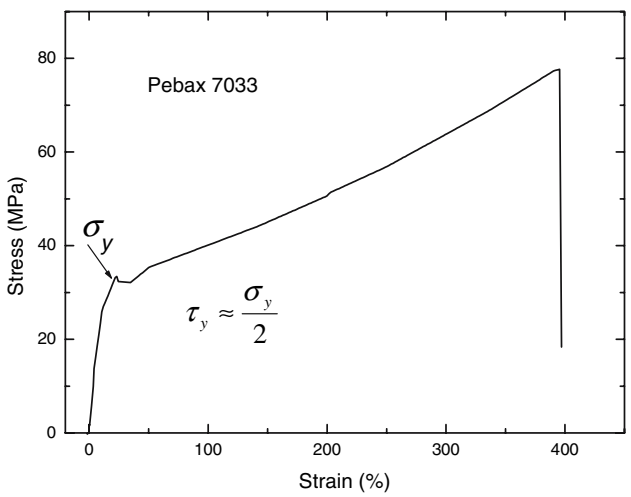

Fig. 1 Stress–strain curves for Pebax 7033. The method of estimating shear yield stress, τ_y is indicated

Table 1 Surface treatments used for PPTA fibers (Aramid–Twaron 2200) for single fiber model composites for fragmentation tests using Raman spectroscopy

Surface treatment	Abbreviation
No surface modifications	AS
Methacryloyl chloride	MC
Succinyl chloride	SC
Argon gas plasma treatment	Plasma 1
Oxygen gas plasma treatment	Plasma 2
Nitrogen gas plasma treatment	Plasma 3
Ammonia gas plasma treatment	Plasma 4
N-vinyl pyrrolidone UV polymerised	NVP
(Neopentyl(diallyl)oxy, tri(N-ethy1enediamino)ethyl titanate (Lica 44)	Li44
Neopentyl (diallyl)oxy, tri(m-amino)phenyl zirconate	NZ97

transferred to 1 L of water containing 20 g sodium hydroxide and 5 g non-ionic surfactant and stirred for 30 min. This process was necessary to neutralise any unreacted chloride as well as to produce fiber disentangling. Wet fibers were filtered, repeatedly washed with deionised water and dried for 2 h in an air-circulating oven at 80 °C. The aramid fibers were washed with a NaOH solution after the chemical grafting. In this way, all free chloride end groups were hydrolysed. The fibers therefore remained non-reactive towards the PA component in the Pebax matrices and the effect induced is solely that of enhancing interactions, such as hydrogen bonds, between the fibers and the matrices in the composites.

Plasma treatment was also carried out using a PS1010 plasma reactor from 4th State Inc., USA. The plasma was generated by a 150 kHz capacitively coupled discharge in a cylindrical chamber using a reactor power of 10 W, a pressure of 0.25 torr, and a gas flow rate of 20 standard cm^3 min^{-1}. Samples were placed in the chamber that was evacuated to a pressure of 10^{-4} torr prior to the admission of the gas. After the plasma treatment, the samples were left in flowing gas for 15 min before the chamber was evacuated and air admitted. The Twaron 2200 PPTA fibers were treated with argon (Plasma 1), oxygen (Plasma 2), nitrogen (Plasma 3) and ammonia / nitrogen (Plasma 4).

N-vinyl-2-pyrollidinone (NVP) was grafted onto the aramid fiber surface using a photo-polymerising procedure. The extent of polymerisation was controlled by varying the irradiation time. The UV lamp used was a Philips HPM15 (2 kW) at a distance of 15 cm from the sample. Benzophenone (Sigma Aldrich) was used as an initiator (hydrogen abstractor), and Irgacure 184 (Ciba Speciality Chemicals) was used as a cross-linking agent.

Coupling agents and adhesion promoters represent a group of speciality bifunctional compounds that can react chemically with both the substrate and the adhesive. The term "coupling agent" refers generally to additives that work on fillers or reinforcements within a resin matrix to improve their properties. Organometallic coupling agents based on zirconium or titanium have been shown to offer a wider compatibility with aramid fiber than the more widely used organosilanes [10]. Lica 44 ((neopentyl(diallyl)oxy, tri(N-ethy1enediamino)ethyl titanate) and NZ97 (neopentyl(diallyl)oxy, tri(m-amino)phenyl zirconate) from Kenrich Petrochemicals Inc., USA were used as the coupling agents. About 1% w/w of the coupling agent was added to a solution of HPLC grade methyl pyrollidinone and aramid fibers were added. The fibers were soaked for 18 h then washed with solvent and dried in an air-circulating oven at 80 °C for 2 h.

Single fibers of Twaron 2200 were prepared for mechanical testing on a card-type fiber rig as described elsewhere [7]. The specimens were conditioned in a temperature-controlled room at 50 ± 5% humidity and 23 ± 2 °C for 7 days in order to allow the adhesive to completely cure prior to testing. The mechanical properties for all specimens (10 specimens per sample) were determined using an Instron 121 universal testing machine following ASTM D3379-75 with a cross-head speed of 1 mm/min for all gauge lengths. The stress at break (σ_f*), strain at break (ε_f*), and modulus (E_f) of the fibers were recorded. The modulus was determined from the initial slope of the stress–strain curve up to 0.5% strain.

Equipment

A Renishaw 1000 Raman imaging microscope was used to record the spectra of the fiber monofilaments using the near IR 785 nm red line of a diode laser. A 50× objective lens of an Olympus BH-2 optical microscope was used to focus the laser beam on the specimen surface (spot size ~2 μm diameter) and to collect 180° back-scattered radiation. A highly-sensitive Renishaw charge-coupled device (CCD) camera was used to collect the Raman spectra. The degree of peak shift and peak broadening under stress of the 1,610 cm^{-1} PPTA Raman band, corresponding to the vibration of the backbone *p*-phenylene ring [6] were determined. The digital data were processed on a computer with the Renishaw analysis software in which a mixed Gaussian–Lorentzian curve fitting procedure was used to determine the peak position and width.

Microcomposite manufacture

Single fiber model composites were prepared by sandwiching a fiber of known length between two films of Pebax 7033. Pebax films of 200 μm thickness were prepared using a Mooney Plastometer Compression Press with the platens heated to 200 °C. The Pebax films were

cooled slowly to room temperature. Typical initial fiber lengths in the fragmentation samples were of the order of 3.0 mm.

Results and discussion

Mechanical properties of surface modified Twaron 2200 fibers

The mechanical properties of the Twaron 2200 fiber subjected to various forms of surface modification are shown in Table 2. It was found that surface modification did not alter the mechanical properties to any appreciable level. In terms of plasma treatment, our findings followed that of several other researchers such as Kupper and Schwartz [11] who used several types of plasma treatments in order to modify the surface of an aramid fiber. Similarly, Brown et al. [12] found that plasma treatment (ammonia, nitrogen, oxygen, carbon dioxide or argon) did not affect the mechanical properties of the aramid fibers.

It is known also that direct exposure of aramid fibers to UV light can lead to gradual strength loss of an unprotected yarn [13]. Brown et al. [14] investigated the light sensitivity of Kevlar 49 (aramid) in terms of yarn strength and polymer degradation. It was found that there was about a 50% reduction in strength after 100 h exposure from a 1,000 W Philips HPL-N mercury vapor fluorescent lamp. They also found that strength loss must be accompanied by polymer degradation via chain scission in the skin region of the Kevlar filaments. Kevlar is sensitive in the 300–340 nm wavelength region, however, despite the sensitivity of aramid fibers to UV radiation, the effect of exposing a Twaron 2200 fiber to 2 min of UV radiation using a Philips HPM15 (2 kW) UV lamp at a distance of 15 cm from the sample did not appreciably affect the mechanical properties. Thus, the application of the UV polymerised NVP coating on the Twaron 2200 fiber did not significantly alter mechanical properties.

Table 2 Mechanical properties of surface-modified Twaron 2200 fibers

Fiber treatment	Extrapolated value of E_f (GPa)	Extrapolated value of σ_f* (GPa)	Extrapolated value of ε_f* (%)
AS (as-received)	136.2 ± 5.4	3.6 ± 0.2	2.6 ± 0.2
MC	133.3 ± 4.3	3.7 ± 0.1	2.5 ± 0.2
SC	129.0 ± 5.3	3.4 ± 0.3	2.6 ± 0.1
Plasma 1	135.2 ± 4.2	3.7 ± 0.3	2.5 ± 0.2
Plasma 2	133.7 ± 5.2	3.3 ± 0.3	2.4 ± 0.1
Plasma 3	134.2 ± 3.1	3.5 ± 0.2	2.5 ± 0.1
Plasma 4	129.0 ± 4.7	3.5 ± 0.1	2.6 + 0.2
NVP	140.1 ± 6.1	4.0 ± 0.3	2.5 ± 0.2
Li44	134.3 ± 3.4	3.5 ± 0.2	2.6 ± 0.1
NZ97	135.3 ± 4.3	3.6 ± 0.1	2.5 ± 0.2

Single fiber deformation and Raman spectroscopy

A Raman spectrum (from 1,350 cm^{-1} to 1,900 cm^{-1}) of the fiber Twaron 2200 in a Pebax 7033 matrix is shown in Fig. 2. The Twaron 2200 fibers give a well-defined Raman spectrum and the peaks have been assigned by Kim et al. [15]. Each peak in the Raman spectrum cannot be attributed to a single mode of molecular deformation but is the result of many. The main peak of interest is that measured at 1,610 cm^{-1} that can be attributed mainly to the asymmetric deformation of the phenylene ring structure and the stretching of the C–C bonds within the phenylene ring. As the *p*-phenylene ring makes up a large portion of the backbone of the polymer chain, and the rigid rod polymer chains of Twaron 2200 are aligned along the fiber axis, it would be expected that any stress applied to the fiber would result in molecular deformation of the backbone including the *p*-phenylene ring. It was found that the peaks shift to lower wavenumber under tensile deformation, with the 1,610 cm^{-1} peak being the most prominent. It is clear that the 1,610 cm^{-1} Raman band of the aramid fiber is well defined and unperturbed by being in the Pebax 7033 matrix. It can also be seen that there is very little fluorescence occurring in the PPTA-Pebax 7033 composite using the near IR 785 nm laser. It was also found that there were no discernable Raman peaks in the 1,610 cm^{-1} region of the virgin Pebax 7033 matrix. The literature value [6] of stress-induced peak shift of –4 cm^{-1}/GPa was used to convert Raman band shift to fibers stress in the subsequent investigation.

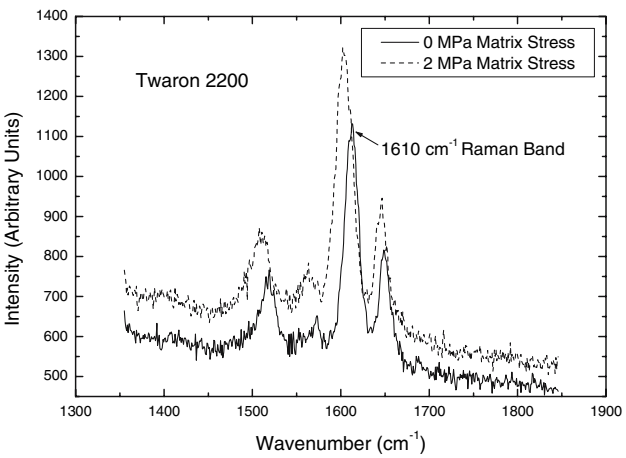

Fig. 2 The shift of the Raman bands (1,350–1,900 cm^{-1}) at different strain levels for a single aramid Twaron 2200 fiber embedded in a Pebax 7033 matrix. Of particular interest is the strong 1,610 cm^{-1} Raman band of the aramid fiber

Stress mapping of single fiber composites

The stress transfer profile of a single Twaron 2200 AS fiber in a Pebax 7033 matrix was determined using Raman spectroscopy at varying levels of stress applied to the single fiber composite as shown in Fig. 3. It is seen that at 0 MPa applied stress, the fiber ends are in slight compression, which is as a result of the different coefficients of thermal expansion, resulting in the matrix compressing on cooling from its molten state. At a matrix stress of 3 MPa, there appears to be good elastic stress transfer from the fiber ends up to a plateau indicating an intact interface. This type of stress profile is in good agreement with the shear lag theory as proposed by Cox [16] for a perfectly-bonded interface.

Upon loading to a higher stress (6 MPa), the fiber breaks twice, resulting in three fragments of similar length. At a higher applied stress again of 17 MPa (not shown in Fig. 3 to aid clarity of presentation), it was found that the middle fragment breaks at around its mid-point resulting in overall, four fragments from the original fiber length. The shape of the fragments corresponded to the triangular shape predicted by Kelly and Tyson [17], in their fully debonded model. It was found that there was some evidence of stress transfer across the fiber ends that is shown in detail in Fig. 3. It should be noted, however, that stress transfer across the fiber ends is assumed not to occur in conventional shear lag analysis [16–19], which is the reason why data were fitted using a cubic spline fit.

The interfacial shear stress (ISS) was determined from the axial stress profiles using a force balance [19]. At 6 MPa matrix stress, the ISS (Fig. 4) shows a plateau from

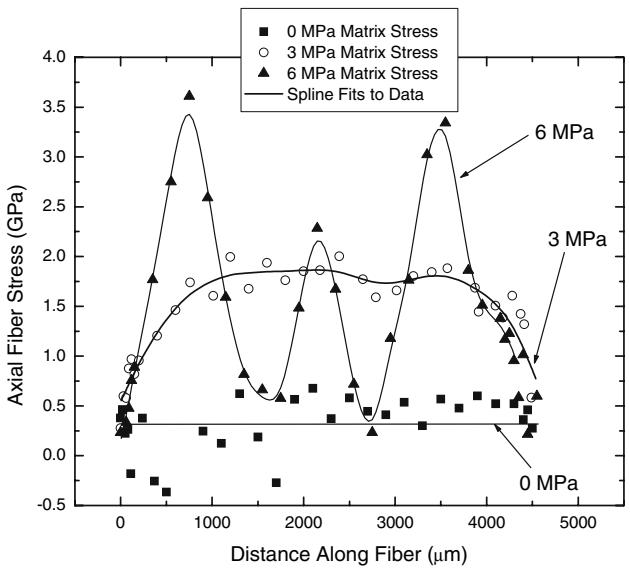

Fig. 3 Axial fiber stress distribution for a typical single fiber composite consisting of an as-received Twaron 2200 (PPTA AS) fiber embedded in the Pebax 7033 matrix

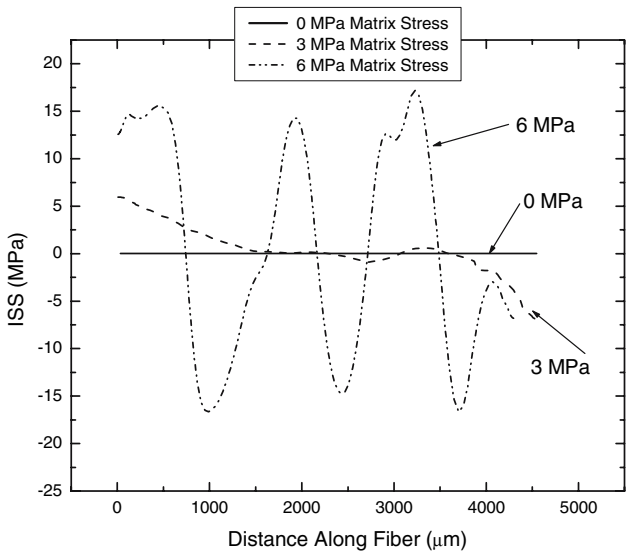

Fig. 4 Interfacial shear stress distribution for a typical single fiber composite consisting of an as-received Twaron 2200 (PPTA AS) fiber embedded in the Pebax 7033 matrix

the LHS fiber end lasting for about 380 μm that occurs due to debonding. This is further reinforced by the axial stress profile of the first fragment at 6 MPa applied stress (Fig. 3) having a linear slope corresponding to that of a full-debonding model as predicted by Kelly and Tyson [17] This model assumes a triangular shape for the entire fragment length, with the maximum axial stress in the centre of the fiber. The derived interfacial shear stress from the spline fit of the stress data, shown in Fig. 4 reaches a maximum of 15 MPa at 6 MPa applied stress, which occurs at the fiber end. As the matrix stress is increased further, the matrix in the interfacial region undergoes debonding. The maximum ISS remains at an almost constant value for each load level, in addition, the ISS remains at a constant value for some distance along the fiber before dropping; this distance generally increasing as the matrix stress is increased. This behavior is characteristic of stress transfer by frictional slip.

The debond length that occurs at the LHS at a matrix stress of 6 MPa is 380 μm. Generally, it is found that the frictional transfer stress would be much lower than the yield stress of the matrix material [20] that in the case of the Pebax matrix used is of the order of 16 MPa ($\approx\sigma_y/2$, Fig. 1).

Figure 5 shows in greater detail the axial fiber stress versus distance along the fiber for a fragment from Fig. 3 at an applied stress of 17 MPa. Figure 6 shows the corresponding ISS curves derived from the cubic spline fits of the stress data for the same fragment. It appears that both fiber end regions show some degree of elastic stress transfer and a correspondingly higher ISS than for debonding. Since it was found from Figs. 3 and 4 that

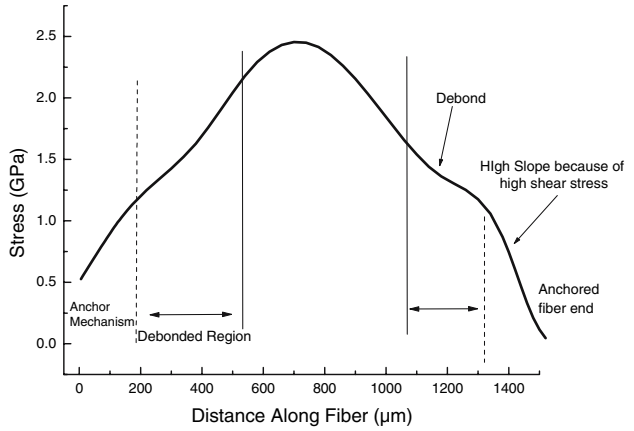

Fig. 5 Stress distribution for a fragment in a PPTA AS fiber embedded in a Pebax 7033 single fiber composite at a matrix stress of 17 MPa (Spline fit of the data points)

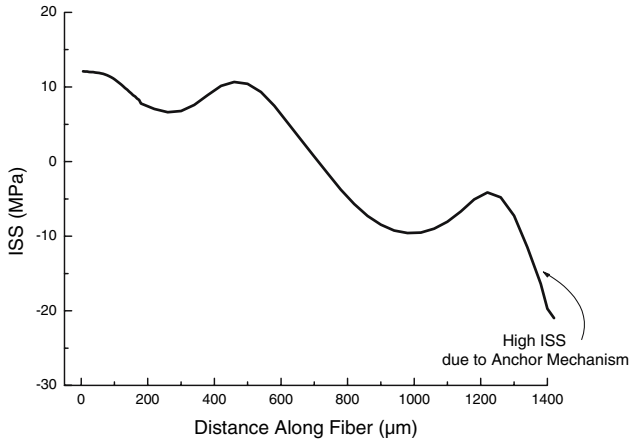

Fig. 6 ISS plot for a fragment in a PPTA AS fiber embedded in a Pebax 7033 single fiber composite at a matrix stress of 17 MPa

debonding took place at lower matrix stresses, it could be argued that this is an apparent "recovery" of the interface. This "recovery", however, is due probably to an "anchoring mechanism", where the fiber end is of a larger cross-sectional area than that of the rest of the fiber as shown schematically in Fig. 7. The fiber end pulls though the matrix after debonding causing a void, until the frictional resistance increases between the fiber end and matrix, and the fiber pull-out ceases.

Visual observations

The Olympus BH2 optical microscope of the Raman spectrometer was used to map visually fiber deformation occurring within the Aramid–Pebax single fiber composite system undergoing fragmentation (Fig. 8). It can be seen that there is some apparent "fraying" where the fiber break occurred but no clear break can be seen. The aramid fiber breaks referred to in this work are termed "apparent

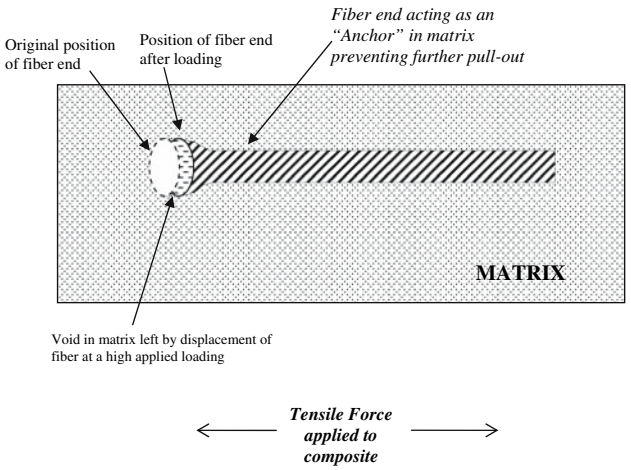

Fig. 7 Proposed "anchor effect" in a fragmentation test sample

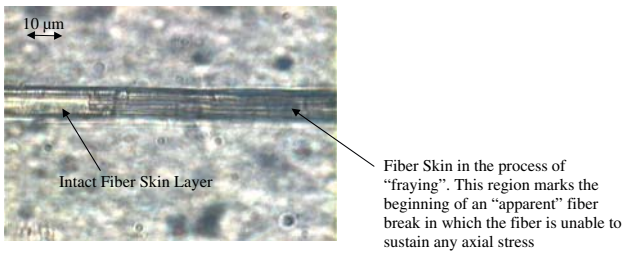

Fig. 8 Optical micrograph of Twaron 2200 fiber in a Pebax 7033 single fiber composite in the region of a fiber break

breaks". This is because there was no visual evidence of clean fracture surfaces as would be the case if the fibers were carbon or glass. This is one of the reasons why aramid fibers were seen as not suitable for the classical fragmentation test, in which the fragment lengths are counted using optical microscopy once fragmentation has reached its saturation state. With the use of Raman spectroscopy, it is possible to ascertain the actual effective lengths of the fragments, by measuring the corresponding axial fiber stress profiles in the fiber. It is clear from the micrograph shown in Fig. 8 that the "apparent breaks" seem to be caused by fiber skin failure. As was shown, a fiber break in an aramid fiber is difficult to assess optically with the fiber skin fibrillating and with the core of the fiber still intact. As a result of the break, however, the ability of the fiber to support load and reinforce the matrix is lost, as in the case of clean breaks in carbon and glass fibers.

Typical stress transfer in a surface modified Twaron 2200 fiber—Pebax 7033 model composite

Axial fiber stress profiles and their corresponding ISS profiles for NVP treated PPTA fiber is shown as a typical example for improved stress transfer response for an

aramid fiber in a Pebax 7033 matrix in Figs. 9 and 10 respectively. It was found that NVP treatment of the Twaron 2200 PPTA fiber did not alter the Raman spectrum or influence the reproducibility of the 1,610 cm^{-1} Raman band.

Figure 9 shows the axial fiber stress profile of a NVP UV polymerised treated PPTA fiber and it can be seen that very high fiber stresses are reached. The average fracture stress for a Twaron 2200 AS fiber was found to be of the order of 3.6 GPa (Table 2). However, since the fiber fracture stress is controlled by the surface integrity, it is possible that the surface treatment has produced a fiber with a much improved skin structure, thus reducing the number of flaws, such that the fiber is able to withstand higher stresses.

As the matrix stress is increased up to 10 MPa, a typical axial fiber stress profile results, comparable to the fully bonded model as proposed by Cox [16], in which an elastic stress distribution from the fiber ends to a plateau along the length of the fiber occurs. As the applied stress is increased further to 13 MPa, the fiber breaks around its mid-point, resulting in two fragments. The axial fiber stress distribution still follows the Cox prediction for a fully bonded system, suggesting that the interface is still intact. At a higher stress of 16 MPa, the first two fragments formed at 13 MPa break at their mid-points, thus resulting in four fragments along the original fiber length. There is some debonding at the fragment ends and this debonding is further shown when the applied matrix stress is further increased and the axial fiber stress profile becomes triangular, which follows the Kelly–Tyson prediction for debonding [17].

The average maximum ISS (shown by the horizontal dashed lines in Fig. 10) derived from the axial stress profile is of the order of 20 MPa. The ISS is somewhat higher than the shear yield strength of the matrix material

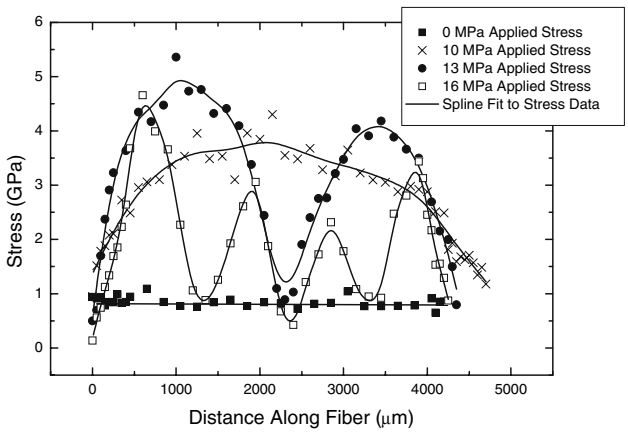

Fig. 9 Axial fiber stress distribution for a NVP Treated PPTA fiber in a Pebax 7033 single fiber composite

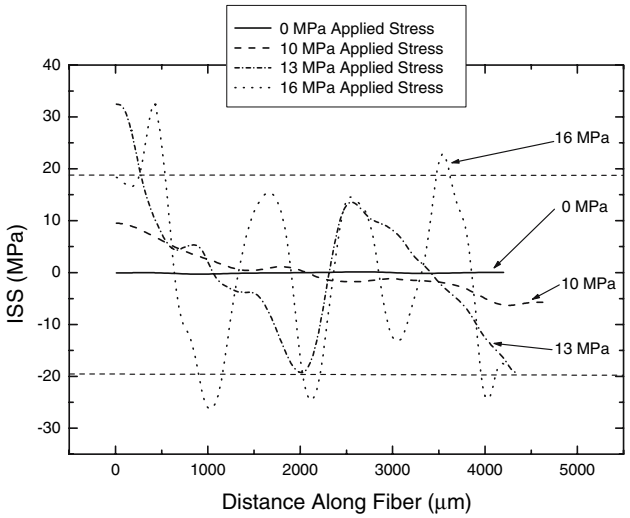

Fig. 10 Interfacial shear stress distribution for a NVP Treated PPTA fiber in a Pebax 7033 single fiber composite

(ca. 16 MPa), but this could be a localized effect of improved interface, and a corresponding interaction between the PPTA fiber, the NVP interphase and the Pebax 7033 matrix. Strain hardening of the matrix after yield as seen in Fig. 1 could also lead to increasing ISS values at higher strains.

Table 3 shows a summary of the main findings from the fragmentation tests of the single fiber reinforced composite samples of surface treated aramid Twaron 2200 fibers in the Pebax 7033 matrix. The maximum axial fiber stresses and strains are given, along with the maximum average interfacial stress and average fragment length. Calculation of the ISS data was conducted using the force balance assumption [19] on the spline fits of the axial stress profiles.

Table 3 Summary of observations seen from the fragmentation test using Raman spectroscopy

Treatment	Max fiber stress (GPa)	Max fiber strain (%)	Average max ISS (MPa)	Average fragment length (μm)
AS	3.2	2.0	15 ± 1.1	1,450 ± 155
MC	5.5	3.3	20 ± 1.3	900 ± 65
SC	3.7	2.25	15 ± 1.5	1,100 ± 65
Plasma 1	3.9	2.3	23 ± 2.0	400 ± 85
Plasma 2	3.5	2.3	14 ± 2.2	N/A (NFS)
Plasma 3	3.5	2.0	20 ± 1.8	720 ± 80
Plasma 4	3.0	1.8	18 ± 2.0	940 ± 65
NVP	4.7	3.15	20 ± 1.5	900 ± 40
Li44	3.75	2.25	13 ± 1.0	1,400 ± 75
N97	3.2	1.75	13 ± 1.2	1,600 ± 80

NFS—Not fully stressed for all breaks to occur

Figure 11 shows the relationship between the ISS and the reciprocal of the fragment length. Using this analysis, ISS determination using Raman spectroscopy can be analyzed using techniques similar to the classical fragmentation method. Long fragments correspond to a weak interface and shorter fragments to a stronger one [21].

It is clear that the coupling agents (NZ97 and Li44) did not improve the stress transfer between the matrix and the fibers. The average fiber fragment length was comparable to that of the as-received Twaron 2200 fiber, but the maximum amount of stress the fragments were able to transfer was far lower. The MC and NVP treated fibers showed effective stress transfer after fragmentation had occurred (3.0 and 2.8 GPa axial fiber stress) while the plasma 1 (Argon) treated fibers had the lowest fragment length and the strongest interface.

Observations on interfacial stress transfer in aramid reinforced Pebax composites

Aramid fibers fail by axial fibrillation which makes the measuring the ISS of the single fiber composite by the fragmentation test, using conventional techniques, quite difficult since the fiber breaks are not easy to locate. Drzal [22] proposed to count the number of regions exhibiting axial fracture (in his study they appeared with a high degree of regularity in spacing). Pisanova et al. [23] believed that their results using the single fiber composite fragmentation test method were not as reliable as other micromechanical methods. The use of Raman spectroscopy, however, for the fragmentation test used in this research has proved to be an accurate method of determining the fiber breaks and an effective data acquisition method to assess the stress profiles of the fibers and to calculate the derived ISS.

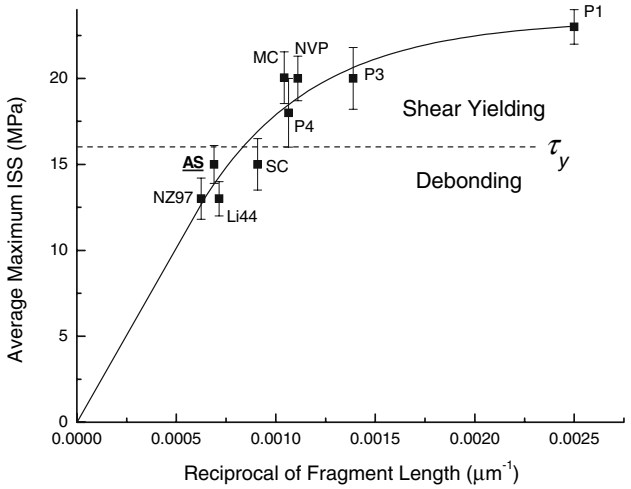

Fig. 11 Average maximum ISS versus average fragment length for Twaron 2200 aramid fibers with various surface treatments embedded in a Pebax 7033 matrix. (Data points taken from Table 3)

The estimated shear yield stress of Pebax 7033 is ≈16 MPa. It was possible to examine the influence of particular fiber sizings on the local interphase and the corresponding interfacial shear stress. It was seen in Fig. 11 that for some samples, the ISS plateau that occurred at a high matrix stress equal to that of the shear yield stress of the neat resin. It would seem that for most samples, stress transfer is limited by yielding of the matrix. At higher applied stresses, however, full debonding of the fiber or fragment ends resulted, and stress transfer was by friction. The idea of local yielding is supported by the work of Gu et al. [24] and Huang and Young [25] using the Raman spectroscopy technique for fiber fragmentation in carbon/epoxy single fiber composites, Huang and Young found that the maximum ISS approximately equals the shear yield stress of the neat matrix.

This does not explain, however, the reason why for some samples such as the Plasma treatment and NVP treated PPTA single fiber composite samples were found to have a ISS somewhat higher than the shear stress of the material (Fig. 11). These ISS values were repeatable to ±2 MPa. Melanitis and Galiotis [26] reported from their Raman experiments on a fragmented carbon fiber in an epoxy matrix that the ISS can be higher than the shear yield stress of the neat matrix. They reported an ISS of 66 MPa, whereas the shear yield stress of the neat matrix (in this case epoxy) was 35 MPa. They explained this disagreement by use of the *interphase* concept as proposed by several researchers [27, 28] The interphase is a region close to the fiber/matrix interface in which it is assumed that the chemical composition of the matrix is different from that of the bulk matrix [29]. Consequently the interphase has mechanical properties different from the bulk. This argument is quite plausible considering the evidence of varying levels of transcrystallinity occurring in the vicinity of the fiber, dependent on the type of fiber surface modification (Coffey AB, unpublished). It would also explain the reason why the Plasma- and NVP-treated fibers have an ISS greater than the shear strength of the Pebax 7033 matrix.

For the Plasma 1 treatment, the interphase region in which there is an improved ISS is probably due to improved surface contact area of the Plasma 1 (argon) treatment. Since inert gases such as argon exist in their monatomic state, their reaction with the fiber surface is a kinetic energy transfer, or in simple terms, a molecular-scale sand blasting process. Thus the likelihood of any contaminants on the fiber surface would be diminished, therefore improving any potential interface with a matrix material. In contrast for the NVP treated fibers, increased hydrogen bonding with the polyamide component of the Pebax matrix could have resulted.

Conclusions

Raman spectroscopy has been used successfully to investigate, using a fragmentation test, the variation of Twaron 2200 aramid fiber stress and the interfacial adhesion along the length of the single-fiber embedded composites with an extensible thermoplastic elastomer (Pebax 7033) matrix. In previous studies using glassy polymeric resins with aramid fibers, it had not been possible to fragment the fibers because of the high failure strain of the fiber. It had only been possible to fragment aramid fibers by employing Kevlar 149 [30] which has a lower strain to failure than conventional aramids.

It was possible to detect the fiber breaks in the Twaron 2200 fibers using Raman spectroscopy and a valuable insight to interfacial stress transfer between aramid fibers and the ductile thermoplastic elastomer matrix was achieved. It would not have been possible to determine accurately the number and position of fiber breaks in the aramid fibers using conventional fragmentation techniques.

The interfacial shear stress between a non-treated, as-received aramid fiber (PPTA AS) and the Pebax 7033 matrix was found to equal or even exceed that of the shear strength of the matrix material, suggesting a good interface. Fiber surface modification showed some improvement in increasing the effectiveness of the interfacial, especially in terms of reducing the critical fiber fragment length, which is a measure of good interfacial adhesion from the classical fragmentation micromechanics theory.

Acknowledgments The authors wish to thank the Marie Curie Fellowship Scheme who funded this work.

References

1. Coffey AB, Brazier A, Tierney M, Gately AG, O'Bradaigh CM (2003) Comp Part A 34:535
2. Rallis G, Tarantili PA, Andreopoulos G (2000) Adv Comp Letters 9:127
3. Huang Y, Young RJ (1994) Comp Sci Tech 52:505
4. Gu XH, Young RJ, Day RJ (1995) J Mater Sci 30:1409
5. Penn L, Bystry F, Karp W, Lee S (1985) In: Ishida H, Kumar G (eds) Molecular characterisation of composite interfaces. Plenum Press, New York, p 93
6. Young RJ (1995) J Text Inst 86:360
7. Eichhorn SJ, Young RJ (2004) Comp Sci Tech 64:767
8. Ciba-Geigy, UK – LY5052 and HY5052, Data sheet
9. Andreopoulos AG (1989) J Appl Polym Sci 38:1053
10. Montes S, Personal Communication, Kenrich Petrochemicals Inc., USA
11. Kupper K, Schwartz P (1991) J Adh Sci Tech 5:16
12. Brown JR, Chappell PJC, Pitt WG, Lakenan JE, Strong AB (1993) J Appl Polym Sci 48:845
13. Yang HH (1993) Kevlar Aramid Fiber, EI du Pont de Nemours & Co., J. Wiley & Sons, NY
14. Brown JR, Browne NM, Burchill PJ, Egglestone GT (1983) J Text Res 53:214
15. Kim PK, Chang C, Hsu SL (1986) Polymer 27:34
16. Cox HL (1952) Br J Appl Phys 3:72
17. Kelly A, Tyson WR (1965) J Mech Phys Solids 13:329
18. Young RJ, Thongpin C, Stanford JL, Lovell PA (2001) Comp Part A 32:253
19. Kelly A, Macmillan NH (1986) Strong solids, 3rd edn. Oxford University Press
20. Bannister DJ (1996) Ph.D. Thesis, Victoria University of Manchester
21. Tripathi D, Jones FR (1998) J Mater Sci 33:1
22. Drzal LT (1983) 15th Nat. SAMPE Tech. Conf., Azusa, Calif. 15:190
23. Pisanova E, Zhandrov SF, Dovgyalo VA (1992) Euradh '92 Conf. Proc. pp 232–237
24. Gu XH, Young RJ, Day RJ (1995) J Mater Sci 30:1409
25. Huang Y, Young RJ (1995) Composites 26:541
26. Melanitis N, Galiotis C (1993) Proc Royal Soc London A 440A:379
27. Jayaraman K, Reifsnider KL, Swain RE (1993) J Compos Technol Res 15:3
28. Williams JG, Donnellan ME, James MR, Morris WL (1990) Mat Res Soc Symp Proc 170:285
29. Herrera-Franco PJ, Drzal LT (1992) Composites 23:2
30. Wagner HD, Amer MS, Schadler LS (1996) J Mater Sci 31: 1165